Air bubble and oil droplet interactions in centrifugal fields during air-sparged hydrocyclone flotation

M. Niewiadomski*

Department of Metallurgical Engineering,
University of Utah,
Salt Lake City, Utah 84112, USA
E-mail: mmniewia@mines.utah.edu
*Corresponding author

Anh V. Nguyen

Division of Chemical Engineering,
School of Engineering,
The University of Queensland,
Brisbane, Queensland 4072, Australia
E-mail: Anh.Nguyen@eng.uq.edu.au

J. Hupka

Department of Chemical Technology,
Gdansk University of Technology,
80-952 Gdansk, Poland
E-mail: jhupka@chem.pg.gda.pl

J. Nalaskowski and J.D. Miller

Department of Metallurgical Engineering,
University of Utah,
Salt Lake City, Utah 84112, USA
E-mail: Jakub.Nalaskowski@mines.utah.edu
E-mail: Jan.Miller@mines.utah.edu

Abstract: The interactions of air bubbles and oil droplets in centrifugal flotation have been considered with respect to process conditions present during Air-sparged Hydrocyclone (ASH) flotation. Encounter efficiency of oil droplets with air bubbles has been found to be significantly smaller when compared to encounter efficiency of mineral particles. Collision and sliding contact times have been determined. Collision has been found to be insufficient for successful contact between oil droplets and air bubbles while sliding allows for film rupture depending on specific system conditions. Although the tenacity of oil droplet attachment to an air bubble is believed to be greater than the tenacity of a mineral particle, emulsification makes oil flotation in centrifugal devices with large dissipation of energy inefficient and hence requires the use of high molecular weight polymeric flocculants.

Keywords: centrifugal flotation; froth flotation; oil flotation; dispersed oil; air-sparged hydrocyclone; ASH.

Reference to this paper should be made as follows: Niewiadomski, M., Nguyen, A.V., Hupka, J., Nalaskowski, J. and Miller, J.D. (2007) 'Air bubble and oil droplet interactions in centrifugal fields during air-sparged hydrocyclone flotation', *Int. J. Environment and Pollution*, Vol. 30, No. 2, pp.313–331.

Biographical notes: Marcin Niewiadomski received his MS (1996) in Chemical Technology from the Gdansk University of Technology, Poland, and his MS (2000) and PhD (2005) in Metallurgical Engineering from the University of Utah. His interests include surface chemistry, wastewater treatment, environmental technologies and protection, and computer programming.

Anh V. Nguyen is the BMA Chair and Professor of Minerals Processing in the School of Engineering at the University of Queensland, Brisbane, Queensland, Australia. He received the degrees of BE (Hons, 1987) and PhD (1992) in Mineral Processing from the Technical University of Kosice, Czechoslovakia. His current research interests include intermolecular and surface forces, interfacial rheology of adsorbed surfactants and particles in foam drainage and emulsification, and colloidal hydrodynamics of bubble-particle interactions. He has authored and co-authored over 100 professional publications, including one authored book on colloidal science of flotation.

Jan Hupka is a Professor in the Faculty of Chemistry at the Gdansk University of Technology, Poland. He received his MS (1971) and PhD (1978) in Chemical Technology from the Gdansk University of Technology. His research interests include advanced separation techniques, environmental technologies, applied physicochemistry of surfaces, and waste utilisation. He has authored or co-authored over 300 professional publications.

Jakub Nalaskowski is a Research Associate Professor in the Department of Metallurgical Engineering at the University of Utah. He received his MS (1994) and PhD (1999) in chemical technology from the Gdansk University of Technology. His research interests include applied physicochemistry of surfaces, atomic force microscopy for surface imaging, and surface force measurements and flotation chemistry.

Jan D. Miller is Chair and the Ivor D. Thomas Professor of Metallurgical Engineering at the University of Utah. He received his BS from the Pennsylvania State University, and his MS and PhD from the Colorado School of Mines. At the University of Utah, he has devoted over 30 years to undergraduate and graduate instruction. During this time he has supervised the research of 88 graduate students who have successfully defended their theses. His research covers mainly the areas of mineral processing and coal preparation, specialising in particulate systems, aqueous solution chemistry, and colloid and surface chemistry. He is a member of the Society for Mining, Metallurgy, and Exploration (SME/AIME), the Minerals, Metals, and Materials Society (TMS/AIME), and the American Chemical Society (ACS). He is the recipient of numerous honours and awards, and in 1993 was elected to the National Academy of Engineering.

1 Introduction

Although centrifugal flotation has been implemented in industrial applications only recently, its history already extends over 80 years. The first application of a centrifugal force field in froth flotation can be traced back to 1922, when Peck (1922) constructed a rotating flotation cell. However, at the time when Peck invented the rotating cell, flotation of fine particles was not recognised as an important issue and the cell was not used by industry. The next device for centrifugal flotation was invented 40 years later when Heide (1963) designed a flotation cyclone. Heide's cyclone resembled a conventional hydrocyclone. Air was mixed with the flotation slurry in the feed inlet and the overflow was replaced by a froth collecting cone. Similarly as was the case for the rotating flotation cell, Heide's cyclone has not been applied in industry.

In less than 20 years after Heide designed his flotation cyclone, flotation of fine particles was finally recognised as an important area in mineral processing and it has been realised that relatively slow flotation rates characterising conventional flotation methods could be overcome in centrifugal flotation. This led to the concept of the Air-sparged Hydrocyclone (ASH), which was developed by Miller (1981). The ASH has been applied in froth flotation to both mineral particles and oily substances including dispersed oil. Considerations of air bubble and oil droplet interactions in this study refer to conditions present in ASH. The details of ASH operation can be found elsewhere (Miller, 1981; Kinneberg, 1991).

2 Centrifugal force field

The centrifugal acceleration in 1-inch and 2-inch ASH units has been estimated based on experimental results for swirl flow reported by Kinneberg (1991). The profile of tangential velocity for the swirl layer in a 2-inch cylinder is presented in Figure 1. The tangential velocity significantly drops within the first several centimetres from the inlet and then increases to a certain maximum after which it steadily decreases. The initial sudden drop of the velocity is characteristic of the hydrocyclone header, which is not aerated by the porous tube and does not take part in the actual flotation process. These tangential velocity profiles allow for the estimate of centrifugal acceleration for the 2-inch ASH. Based on these estimations approximate values for 1-inch ASH unit have been determined. Three values are distinguished, maximal centrifugal acceleration in the inlet, maximal acceleration in the aerated section and the lowest centrifugal acceleration in the outlet. Table 1 presents estimated values for centrifugal acceleration in 2-inch and 1-inch ASH units.

Entropic forces responsible for Brownian motion acting on fine oil droplets are important to determine the smallest particle size below which the classical approach to oil droplet encounter and collision with an air bubble can no longer be used. As the size of an oil droplet decreases the entropic force becomes more significant. The ratio between buoyancy and entropic forces can be found from the following formula (Bergeron et al., 1997):

$$\frac{F_b}{F_{kT}} = \frac{2\pi R_{\text{oil}}^4 (\rho_w - \rho_{\text{oil}}) g}{3kT}. \tag{1}$$

Figure 1 Tangential fluid velocity in 2-inch cylinder

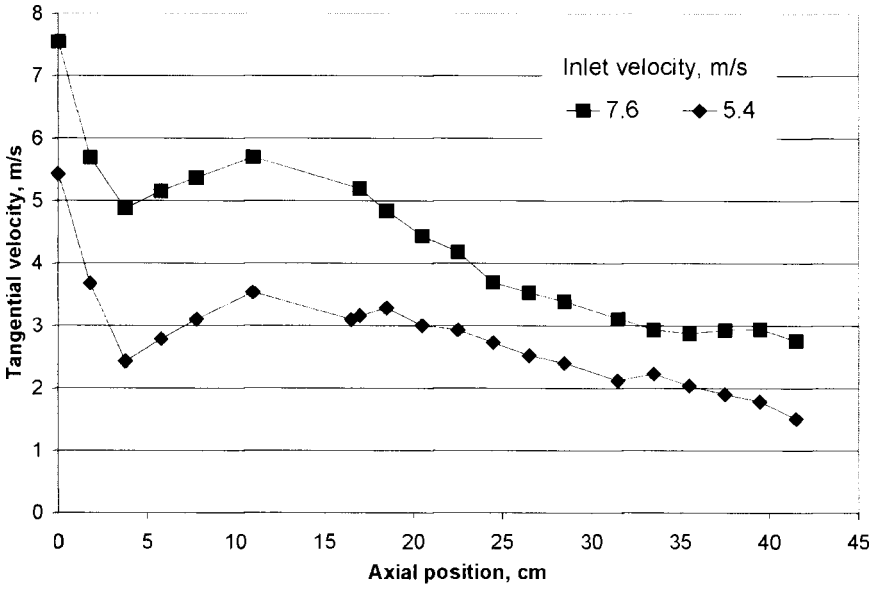

Source: Kinneberg (1991)

Table 1 Centrifugal acceleration in ASH

	Centrifugal acceleration (g)		
Feed flowrate (dm^3/min)	*Inlet*	*Maximum, aerated*	*Outlet*
2-inch ASH unit, 41 cm total cylindrical length			
70.0	229	130	41
55.0	144	57	25
40.0	74	29	12
1-inch ASH unit, 14 cm total cylindrical length			
24.0	803	458	94
21.0	615	301	64
16.2	366	155	37
9.6	128	48	10
6.3	55	20	4

One can assume the critical ratio of oil droplet buoyancy force to entropic force to be one and use equation (1) to determine the critical oil droplet size. The Earth's gravitational acceleration can be replaced by centrifugal acceleration. In the case of mineral oil having a density 842 kg/m^3 the critical droplet diameter as a function of centrifugal acceleration at 298 K is presented in Figure 2. The critical size decreases from 1.8 μm for Earth's gravitational acceleration to 0.34 μm for acceleration 800 times larger.

Figure 2 Critical oil droplet size as a function of centrifugal acceleration

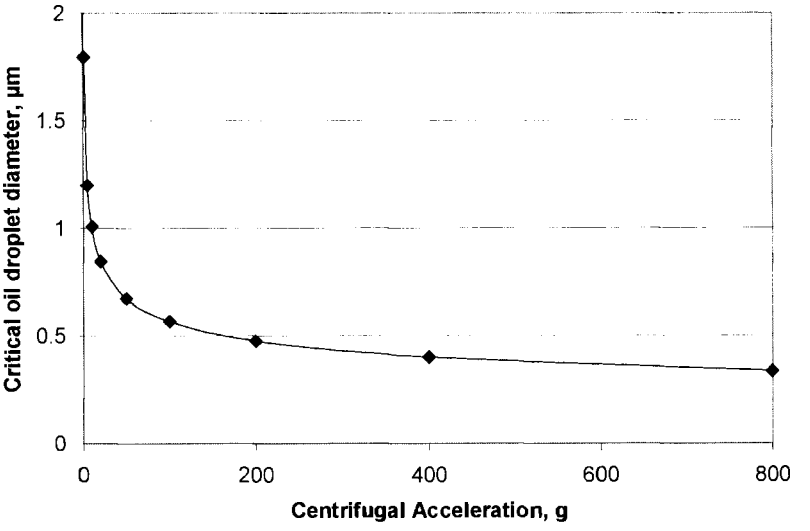

3 Air bubble and oil droplet interactions

It is generally accepted that in centrifugal flotation more coherent air-particle aggregates are required due to a greater possibility for detachment when compared to conventional flotation. However, there is no detailed analysis of phenomena controlling the attachment and detachment of air bubbles and oil droplets. Based on available models for air bubble-mineral particle systems appropriate analysis and calculations for air bubble-oil droplet interactions can be performed.

Two steps in the attachment process can be distinguished: encounter or collision, and intervening film thinning and rupture. Air bubble-particle collisions and attachment have been studied extensively in froth flotation research, but detachment only recently has been investigated in more detail. The fundamentals of bubble-particle aggregate stability were formulated early in the 1930s (Kabanov and Frumkin, 1933; Wark, 1933; Gaudin, 1939). In the 1970s and 1980s Schulze (1977a, 1977b, 1983) further advanced the theory and conducted experimental work pertaining to bubble-particle aggregate stability. It has been shown that bubble-particle detachment is described by highly nonlinear equations. Coupling of capillary and gravity forces has been described in terms of particle size, density and contact angle among many other parameters.

The interactions of air bubbles with oil droplets is considered in this research in three parts:

- encounter
- liquid film thinning followed by rupture/attachment
- detachment.

3.1 Encounter of an air bubble and an oil droplet

Encounter efficiency can be defined as a chance that a mineral particle or oil droplet in the path swept by a rising air bubble approaches its surface so closely that a thin water film is formed. The encounter efficiency is never greater than one.

The efficiency evaluation of air bubble and particle encounter has a rich literature (Schulze, 1989; Dai et al., 2000; Ralston et al., 2002; Nguyen and Schulze, 2004). According to the approach proposed by Schulze there are four major mechanisms responsible for the efficient encounter of an air bubble and a particle: gravity action, interception, inertial impaction and turbulent motions. These four mechanisms are explained in the following paragraphs. One can use this approach to investigate air bubble-oil droplet encounters. The key difference between flotation of mineral particles and oil droplets is that mineral particles have a density greater than that of water whereas oil droplets have a smaller density.

In the case of encounter by the action of gravity, particles in suspension have a certain settling velocity. Gravitational settling causes particles to approach an air bubble from above. As they fall they deviate from water streamlines flowing around an air bubble. In the case of mineral particles they can approach the air bubble in the vicinity of the fore part of the bubble. An oil droplet, however, can not approach an air bubble by gravity action alone since it has less inertia than the surrounding water. Both air bubble and oil droplet rise since they have a lower density than that of water. Nevertheless, an air bubble usually has a greater rise velocity and hence the oil droplet appears to fall on the air bubble similar to a mineral particle only with a smaller relative velocity. The oil droplet initially moves away from the air bubble and approaches when passing around the aft part of the bubble. Due to flow fore-and-aft asymmetry, it can be assumed that the oil droplet will not be able to return to its initial distance from the air bubble. For this reason, the efficiency of encounter by gravity action, E_g, can be approximated as zero. Figure 3 represents the encounter by gravity action of a mineral particle and an oil droplet with an air bubble.

Figure 3 Comparison of encounter efficiency for a mineral particle and an oil droplet with an air bubble in the Earth's gravitational field

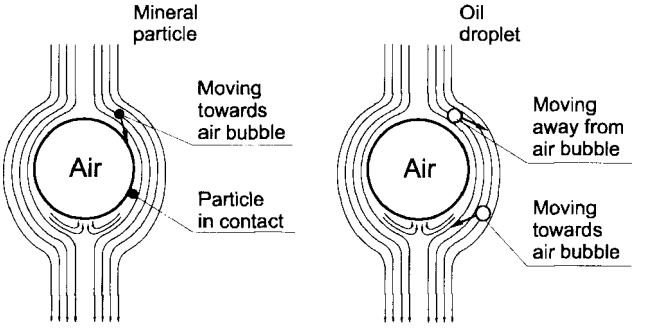

In the case of encounter by interception, a particle or oil droplet is considered to follow water streamlines, however, since it has a certain diameter larger than zero, a sufficiently large particle or droplet can touch the air bubble surface. Density does not play a role in this mechanism and the encounter efficiency by interception of the oil droplet can be found in the same way as the encounter efficiency of a mineral particle.

Both mechanisms, gravity action and interception, can be considered together. One can draw a so-called grazing trajectory for a mineral particle or an oil droplet, which determines the water volume at the front of a rising bubble in which volume all mineral particles or oil droplets encounter the air bubble. It is apparent, that in contradiction to an encounter with a mineral particle, gravity hinders the oil droplet encounter efficiency, and the grazing trajectory for an oil droplet is significantly smaller, see Figure 4.

Figure 4 Comparison of grazing trajectory for a mineral particle and an oil droplet

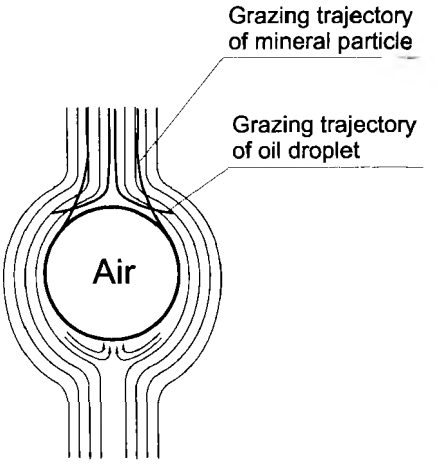

Inertial impaction occurs when a mineral particle or oil droplet cannot follow the curvilinear motion of water due to its inertia. While a mineral particle tends to continue along a straight path, an oil droplet with less inertia than that of water tends to deviate from straight paths yielding to the water stream. In centrifugal flotation inertial impaction plays a significantly greater role compared to gravity action. Similarly as in the case of the encounter by gravity action, densities of specific phases are important. The oil droplet initially moves away from an air bubble, thus it cannot collide when passing the fore part of the air bubble. Efficiency of collisions by inertial impaction, E_{in} can be assumed to be zero.

The theory on encounter by turbulent motion has not been fully developed. The encounter efficiency by this mechanism can be solved using turbulent statistics and was given by Levich (1962). The efficiency decreases with an increase in bubble and particle sizes and increases with an increase in the scale of turbulence, λ_k:

$$E_{\text{tur}} = 18\sqrt{\frac{3}{15}}\frac{\delta}{\rho - \delta}\frac{\lambda_k}{R_b + R_p}. \tag{2}$$

Analysis of the relationship given by Levich indicates that the encounter efficiency can be quite high as the particle density may only be slightly more dense than water. Extrapolating the applicability of equation (2) to oil droplets having a smaller density than that of water one can conclude that the efficiency becomes negative in value. In order to use equation (2) for predicting encounter efficiency of oil droplets, the absolute value of the density difference should be used. Attached oil can form a lens or spread on the bubble surface, see Figure 5.

Figure 5 Oil droplet attached to an air bubble assuming a lens or spreading on the bubble surface

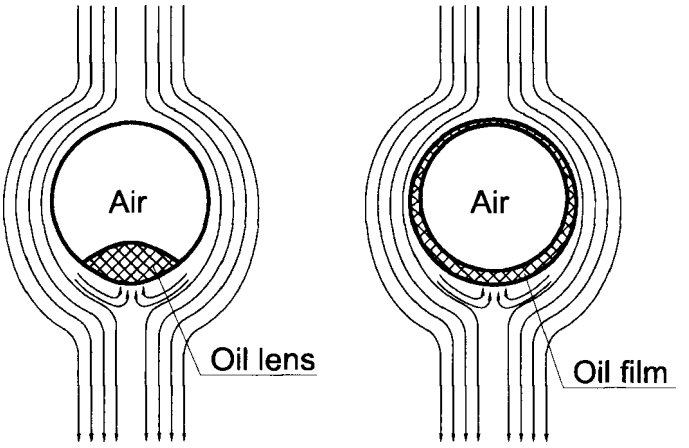

One can draw some general conclusions when comparing mineral particles and oil droplets in turbulent flow conditions. When both the mineral particle and air bubble have smaller sizes than the size of a turbulent eddy, they move in opposite directions within the eddy. Air bubbles tend to locate themselves in the centre of a turbulent eddy, while mineral particles by centrifugation tend to leave the eddy. In the case of an oil droplet, it acts similarly to the air bubble and tends to locate itself in the centre of a turbulent eddy. This phenomenon is believed to enhance the encounter efficiency for oil droplets by turbulent motion. When an air bubble is larger and the oil droplet is smaller than a turbulent eddy, the oil droplet, in contradiction to a mineral particle, can not reach the bubble surface since it stays inside the eddy. In this case, the efficiency of oil droplet encounter is believed to be zero. When an air bubble and oil droplet are both larger than a turbulent eddy, the encounter efficiency of an oil droplet is believed to be enhanced due to the lower inertia of an oil droplet when compared to that of a mineral particle. When an air bubble is smaller and the oil droplet larger than a turbulent eddy, one can consider this situation to be similar to the case in which an air bubble is larger and oil droplet smaller than a turbulent eddy. The encounter efficiency, however, is believed to be about the same. The four cases described above are presented in Figure 6. Summarising, it is very difficult to estimate the actual impact of turbulent motion on the oil droplet encounter efficiency when compared to the encounter efficiency of a mineral particle. However, it is assumed that the overall efficiency due to turbulent fluid motion can be considered to be about the same.

The encounter efficiencies of oil droplets are compared to those of mineral particles for all four mechanisms in Table 2. The overall encounter efficiency, E_c of the air bubble and oil droplet would include efficiency terms for interception and turbulent terms. In the case when one of these two mechanisms is predominant, the overall efficiency may be estimated from equation (3):

$$E_c = 1 - (1 - E_i)(1 - E_{tur}). \tag{3}$$

Figure 6 Mineral particle and oil droplet encounters with an air bubble under turbulent conditions

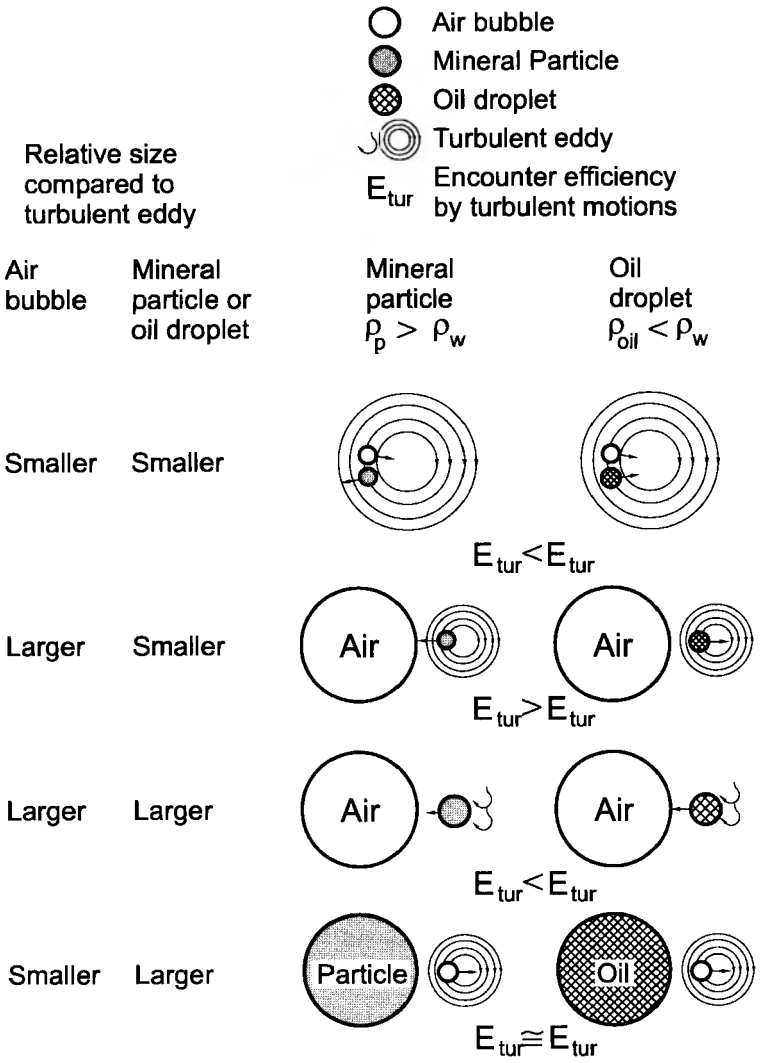

Table 2 Encounter efficiency comparison between oil droplets and mineral particles

Encounter mechanism	*Efficiency of oil droplet encounter compared to efficiency of mineral particle encounter*
Gravity	Zero efficiency
Interception	Reduced by gravity action
Inertial impaction	Zero efficiency
Turbulent motions	About the same

3.2 *Water film thinning between an air bubble and an oil droplet*

After a successful encounter creating an air bubble and oil droplet aggregate, the intervening water film must thin and break. Contact time of the air bubble with the oil droplet significantly influences the possibility of a successful thin film rupture. The time needed for a thin film to break is referred to as the induction time. A mineral particle or oil droplet staying in contact with an air bubble for a time shorter than the induction time will not successfully attach. One can distinguish two models for predicting the contact time, collision and sliding.

There are several theories on collision contact time. Philippoff (1952) created the first model for air bubble-particle interaction and collision time, which considered a cylindrical particle. Evans (1954) further developed the model for a spherical particle. Ye and Miller (1988) and Ye et al. (1989) included the effect of the bubble and particle motions. Scheludko et al. (1976) modified the model by more detailed considerations of the interface geometry, which was further studied by Schulze et al. (1989). The most recent model was derived by Nguyen et al. (1997). The collision contact time can be determined using equations (4)–(10). The relative velocity, V, can be found from rising velocities of air bubbles and oil droplets determined from the equation (9) given by Nguyen for flow conditions of small air bubbles in contaminated water (Nguyen et al., 1997). Equation (9) can be used for oil droplets when the oil density is accordingly taken into account.

$$t_c = \frac{\pi}{\phi}\left\{\frac{R_{\text{oil}}^3\left(\rho_{\text{oil}} + \rho_w/2\right)}{3\gamma_{wg}}\right\}^{1/2} \tag{4}$$

$$\phi = 0.506 + 0.04\ln\frac{R_{\text{oil}}}{L} + \left\{0.041 + 0.03\ln\frac{R_{\text{oil}}}{L}\right\}\ln \text{We} \tag{5}$$

$$0.018 \le \frac{R_{\text{oil}}}{L} \le 0.2 \tag{6}$$

$$L = \sqrt{\frac{\gamma_{wg}}{g\rho_w}} \tag{7}$$

$$\text{We} = \frac{V}{L}\sqrt{\frac{R_{\text{oil}}^3\left(\rho_{\text{oil}} + \rho_w/2\right)}{3\gamma_{wg}}} \tag{8}$$

$$U_r = \frac{2R_{b/o}^2 g(\rho_w - \rho_{g/o})}{9\mu\left(1 + \text{Ar}/96(1 + 0.079\ \text{Ar}^{0.749})^{0.755}\right)} \tag{9}$$

$$\text{Ar} = \frac{8R_{b/o}^3 g(\rho_w - \rho_{g/o})\rho_{g/o}}{\mu^2}. \tag{10}$$

The estimated collision contact times for oil droplets are presented in Table 3. The interfacial tension of oil droplets with the aqueous phase has been assumed to be 30 mN/m.

Table 3 Collision contact time between air bubbles and oil droplets

Oil droplet diameter (μm)	*Acceleration range* (g)	*Air bubble diameter* (μm)				
		10	*20*	*100*	*200*	*600*
		Collision contact time range (μs)				
10	50–800	3–7	4–7	5–8	5–8	6–9
20	10–800	9–23	10–24	12–26	13–26	15–27
60	5–100	–	–	79–131	85–134	93–140

In order to be able to determine if the estimated collision contact times are sufficient for successful air bubble and oil droplet attachment, one has to know the time required for the intervening film rupture. Useful information on rupture times may be found in reports pertaining to oil emulsion based antifoams. It has been indicated that a key role in successful penetration of the air/water interface by oil droplets is a positive entry coefficient (Koczo et al., 1992). When the entry coefficient remains negative, the oil droplet is not capable of entering the air bubble surface unless other factors force the attachment. One can consider fluid turbulent motion to provide the necessary energy for the liquid film rupture. Negative entry coefficients can be observed for systems at high surfactant concentrations when the oil droplet surface is hydrophilic. It has been further indicated that film rupture for an oil emulsion can be accomplished in 2–3 seconds using antifoams containing a small amount of very fine hydrophobic particles (Koczo et al., 1994). Denkov et al. (1999) reported the shortest observed rupture times between 2 ms and 10 ms. Bergeron et al. (1997) showed that smaller droplets need to approach the interface more closely before they can rupture the aqueous thin film, which he also observed for dodecane oil droplets approaching the air/water interface. Taking into account all these reported findings, one can conclude that rupture of the thin aqueous film between an air bubble and an oil droplet is a complex process and a single, simple description cannot be found. Rupture times may vary from a few milliseconds to a few seconds depending on the system composition and in particular if very fine hydrophobic particles are present. For the purpose of determining the efficiency of attachment by collision one can assume a necessary contact time of 2 ms. The calculated longest contact time as shown in Table 3 is 140 μs, which is only 7% of the necessary time of 2 ms. Attachment by collision appears to be impossible or at most very unlikely to occur.

The sliding contact time can be modelled using the expression for particle velocity on the bubble surface. The first equation for predicting sliding contact time was given by Sutherland (1948). Dobby and Finch (1986) corrected this equation assuming that fluid stream lines start to deviate away from the particle surface at a polar position equal to 90°. Yoon and Luttrell (1989) further studied the sliding contact time, though their model does not take into account sedimentation of particles and fore-and-aft asymmetry of the flow passing the bubble surface. The most recent model was developed by Nguyen et al. (1997). Applying the mobile bubble surface model, the sliding contact time can be found using equations (11)–(22). Model parameters M, N, X and Y can be determined for a bubble with a mobile surface using equations (14)–(17). The approximation of ε as the volume fraction of the gas phase can be used in oil ASH flotation, since the flotation slurry is extensively aerated. Most often air flowrate exceeds water flowrate and ε has been assumed to be 0.66 based on typical aeration applied by the authors during ASH oil

flotation experiments. The dimensionless numbers C and C_1 for a bubble with a mobile surface can be calculated from equations (18) and (19). In order to determine the sliding contact time the maximum angle of the oil droplet sliding over the air bubble, φ_m also needs to be determined from equation (22).

$$t_{sl} = \frac{R_{oil} + R_b}{U(1 - B^2)A} \ln\left\{ \frac{\tan(\varphi_m / 2)}{\tan(\varphi_0 / 2)} \left[\frac{\operatorname{cosec}(\varphi_m) + B\cot(\varphi_m)}{\operatorname{cosec}(\varphi_0) + B\cot(\varphi_0)} \right]^B \right\} \tag{11}$$

$$A = \frac{V_S}{U} + \frac{R_{oil}}{R_b} X + \left(\frac{R_{oil}}{R_b} \right)^2 \frac{M}{2} \tag{12}$$

$$B = \frac{R_{oil}}{R_b} \frac{Y}{A} + \left(\frac{R_{oil}}{R_b} \right)^2 \frac{N}{2A} \tag{13}$$

$$X = 1 + \frac{0.0637\ \mathrm{Re}_b}{1 + 0.0438\ \mathrm{Re}_b^{0.976}} + (5.274 - 0.588\ \mathrm{Re}_b^{0.23})\varepsilon^{0.711} \tag{14}$$

$$Y = \frac{0.0537\ \mathrm{Re}_b}{1 + 0.0318\ \mathrm{Re}_b^{1.309}} - \frac{0.0513\ \mathrm{Re}_b^{1.015}\varepsilon^{0.0559}}{1 + 0.0371\ \mathrm{Re}_b^{1.308}} \tag{15}$$

$$M = -1 - 0.267\ \mathrm{Re}_b^{0.781} - (30.431 + 0.951\ \mathrm{Re}_b^{0.777})\varepsilon^{1.426} \tag{16}$$

$$N = \frac{-0.00591\ \mathrm{Re}_b}{1 + 1.105\ \mathrm{Re}_b^{0.334}} - 1.974\ \mathrm{Re}_b^{0.569}\varepsilon^{0.252} \tag{17}$$

$$C = \frac{V_S}{U \cdot f(R)} \tag{18}$$

$$C_1 = \frac{\mathrm{St}}{2 \cdot f(R)} \left(1 - \frac{\rho_w}{\rho_{oil}} \right) \tag{19}$$

$$\mathrm{St} = \frac{2R_{oil}^2 U \rho_{oil}}{9\mu R_b} \tag{20}$$

$$f(R) = \frac{R_{oil}}{R_b} - \left(\frac{R_{oil}}{R_b} \right)^2 + O\left(\frac{R_{oil}}{R_b} \right)^3 \tag{21}$$

$$\varphi_m = \arccos \frac{\sqrt{(X + C)^2 + C_1^2 X^4} - (X + C)}{C_1 X^2}. \tag{22}$$

Sliding contact times for air bubbles ranging in size from 10 μm to 200 μm and oil droplets from 1 μm to 20 μm are presented in Figures 7 and 8. The sliding contact times are estimated for conditions in which the oil droplet buoyancy force exceeded the entropic force and calculations resulted in a positive time. In the case of air bubbles of sizes 10 μm and 20 μm and oil droplets of sizes 1 μm and 2 μm contact times are shorter

than the assumed limiting value of 2 ms at centrifugal accelerations varying from 50 g to 400 g. Air bubbles of size 20 μm and oil droplets 10 μm show sliding contact times between 0.1 s and 1 s. Air bubbles of size 200 μm have longer sliding contact times compared to air bubbles of size 100 μm when interacting with oil droplets of sizes 1 μm and 2 μm. Also when considering bubbles 100 μm and 200 μm in size, a very strong dependence on oil droplet size can be seen. With an increase in oil droplet size sliding contact time decreases as the acceleration increases. The beginning angle also has a significant influence for larger oil droplets, 10 μm and 20 μm.

Considering that thin film rupture times can vary between 2 ms and 3 s, one can conclude that depending on the conditions controlling the actual rupture the attachment efficiency of air bubbles and oil droplets can be large at centrifugal accelerations of up to 100 g or 200 g. However, if conditions are not sufficient and long sliding contact times are needed the efficiency can be extremely low, since estimated times do not reach the required 3 s for any of the air bubble and oil droplet sizes investigated.

Figure 7 Sliding contact time for air bubbles 10 μm and 20 μm in diameter

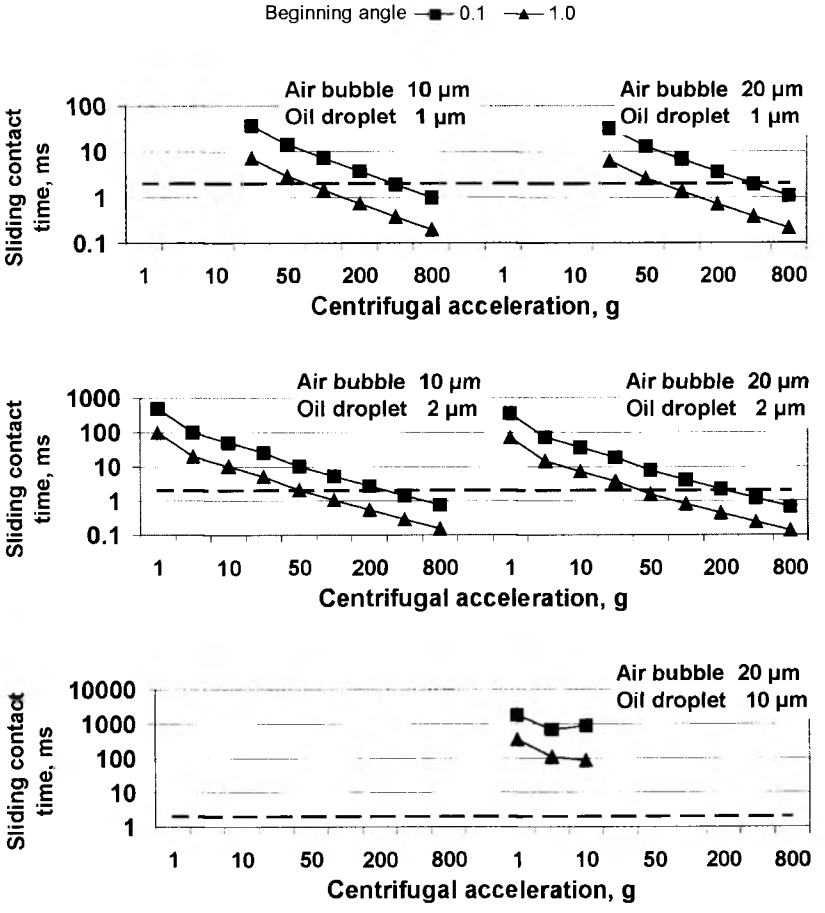

Figure 8 Sliding contact time for air bubbles 100 μm and 200 μm in diameter

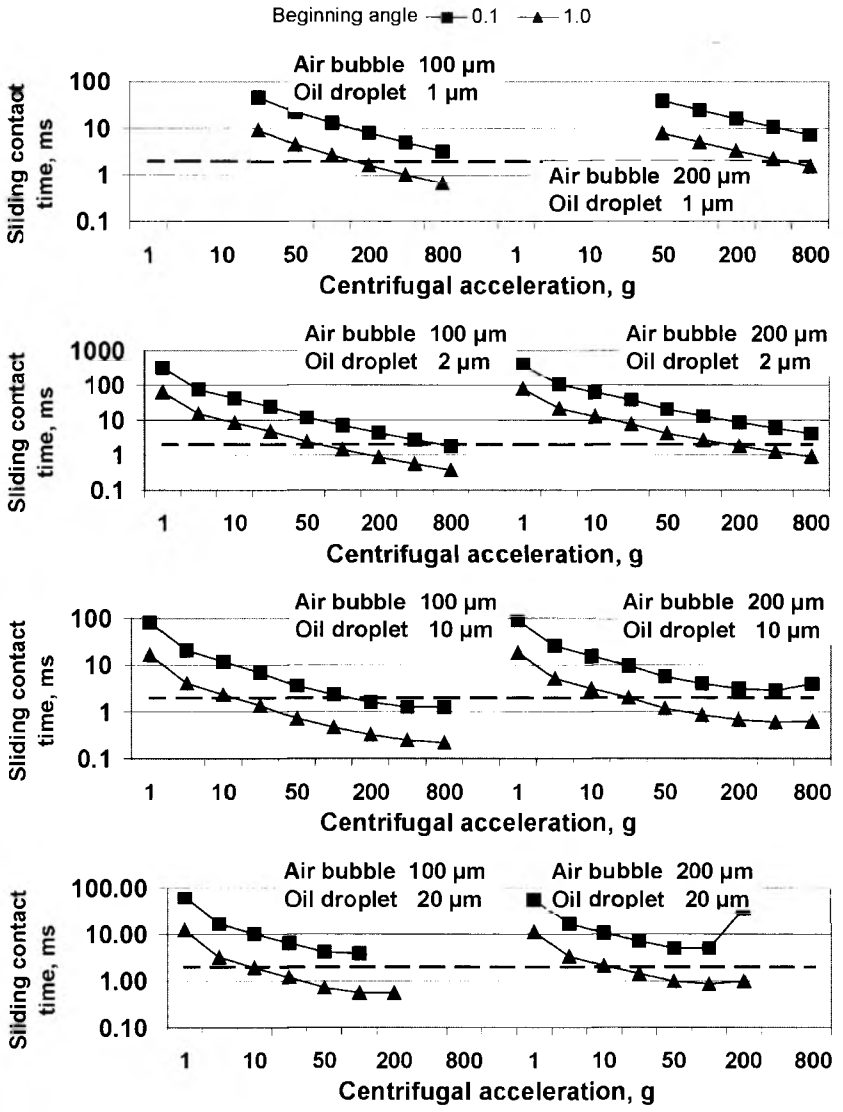

3.3 Attachment tenacity of an air bubble and an oil droplet

An oil droplet can assume one of two possible arrangements when in contact with an air bubble. It can either form a lens, which will occupy the aft bubble surface or spread over the entire air bubble surface, see Figure 5. A list of forces acting on a mineral particle or oil droplet attached to an air bubble in the form of a lens is presented in Table 4. Capillary force tends to attach a mineral particle to an air bubble, but in the case of an oil droplet this force is neutral since oil is in the liquid state. Pressure force in both cases is attaching. Buoyancy, gravity and inertial forces tend to detach a mineral particle but to attach an oil droplet. Drag and turbulent forces tend to detach both a mineral particle and an oil droplet. Detachment of the oil droplet, however, is believed to be the

actual emulsification process. This comparison shows that one can expect the tenacity of an air bubble and oil droplet aggregate to be stronger when compared to that of a bubble aggregate formed with a mineral particle of the same size. The most significant difference is the opposite effects of buoyancy, gravity and inertial forces. Considering the greater air bubble velocity in a centrifugal force field, one can expect a much larger drag exerted on the oil phase attached to an air bubble.

Table 4 Forces acting on an air bubble aggregate with a mineral particle or oil droplet

Force	*Character of the force*	
	Mineral particle ($\rho_p > \rho_w$)	*Oil droplet – lens* ($\rho_{oil} < \rho_w$)
Capillary	Attaching	Neutral
Pressure	Attaching	Attaching
Buoyancy and gravity	Detaching	Attaching
Inertial	Detaching	Attaching
Drag	Detaching	Detaching/emulsifying
Turbulent	Detaching	Detaching/emulsifying

Determining the drag force exerted on the oil lens positioned at the aft part of the bubble surface is very difficult since water flow in that point is expected to be highly turbulent. This turbulent flow may disperse the attached oil lens into multiple smaller droplets provided it has sufficient energy. The oil film spread at the air bubble surface is exposed to a similar water drag, which would be otherwise exerted on the bubble. Considering that the assumed surface energy at the oil/water interface is approximately 50% of the energy at the air/water interface, the emulsification of an oil film appears possible for conditions at which the air bubble maintains its integrity. The calculations of energy dissipation in 2-inch and 1-inch ASH are presented in Table 5. The estimated values can be further compared with the energy needed to split an oil droplet into two equal size smaller droplets, see Table 6.

Table 5 Energy dissipation in ASH

Feed flowrate (dm^3/min)	*Energy dissipation* (J/kg)
2-inch ASH unit, 41 cm total cylindrical length	
70.0	4038
55.0	2041
40.0	803
1-inch ASH unit, 14 cm total cylindrical length	
24.0	14201
21.0	9680
16.2	4460
9.6	955
6.3	273

Table 6 Ratio of energy dissipation to energy required for division of an oil droplet. Surface energy 20 mJ/m^2

	Oil droplet diameter (μm)				
Feed flowrate (dm^3/min)	*1*	*5*	*10*	*50*	*100*
2-inch ASH unit, 71 cm total cylindrical length					
70.0	258	316	578	2706	5368
55.0	130	160	292	1368	2714
40.0	51	63	115	538	1067
1-inch ASH unit, 14 cm total cylindrical length					
24.0	908	1113	2034	9516	18879
21.0	619	759	1387	6486	12868
16.2	285	350	639	2988	5929
9.6	61	75	137	640	1269
6.3	17	21	39	183	363

The dissipation energy in ASH flotation can exceed the energy required for an oil droplet to split into two smaller droplets of equivalent size from 17 to nearly 19,000 times. The energy required to split an oil droplet into two droplets of the same size is greater when compared to the energy needed to split into two droplets of different size. For this reason, the emulsification process occurs with the generation of many smaller droplets, which requires even less energy. Although the tenacity of an air bubble/oil droplet aggregate is believed to be greater than the tenacity of a mineral particle aggregate, the emulsification of attached oil makes oil flotation in centrifugal devices having large dissipation energies not very efficient. For this reason the use of water soluble polymers is necessary to stabilise air bubble/oil droplet aggregates in these turbulent fields.

4 Conclusions

Encounter efficiency in the flotation of oil droplets has been found to be significantly smaller when compared to the encounter efficiency in the flotation of mineral particles. Centrifugal force fields further reduce the encounter efficiency of an air bubble and oil droplet. In the investigated range of air bubble and oil droplet sizes collision contact times have been estimated to be less than 0.14 ms, while calculated sliding contact times depend significantly upon centrifugal acceleration and vary from less than 1 ms to almost 400 ms. Water film rupture times have been reported in the literature to vary from 2 ms to 3 s and one can conclude that collision is not sufficient for successful contact between an oil droplet and an air bubble while sliding allows for rupture depending on specific system conditions. The stability of an air bubble/oil droplet aggregate has been found to be greater than the stability of an air bubble aggregate formed with a mineral particle. However, high energy dissipation in centrifugal flotation devices like the ASH is believed to destroy the air bubble/oil droplet aggregates by emulsification of oil attached to an air bubble.

Reduced encounter efficiency explains why formation of air bubble/oil droplet aggregates requires polymeric flocculants to significantly enhance oil recovery. With the use of water soluble polymers air bubbles do not need to be attached to oil droplets, but can be captured by the three dimensional floc structures formed from oil droplets in the presence of a polymer. Flocculation avoids the problem of sufficient contact time for thin film thinning and rupture. However, large energy dissipation levels still can easily destroy flocs. This turbulence problem in oil flotation is valid for all centrifugal flotation devices in which centrifugal acceleration is achieved by circular fluid motion in a stationary chamber.

References

Bergeron, V., Cooper, P., Fisher, C., Giermanska-Kahn, J., Langevin, D. and Pouchelon, A. (1997) 'Polydimethylsiloxane (PDMS)-based antifoams', *Colloids and Surfaces A*, Vol. 122, pp.103–120.

Dai, Z., Fornasiero, D. and Ralston, J. (2000) 'Particle–bubble collision models – a review', *Adv. Colloid Interface Sci.*, Vol. 85, pp.231–256.

Denkov, N.D., Cooper, P. and Martin, J.Y. (1999) 'Mechanisms of action of mixed solid-liquid antifoams. 1. Dynamics of foam film rupture', *Langmuir*, Vol. 15, pp.8514–8529.

Dobby, G.S. and Finch, J.A. (1986) 'A model of particle sliding time for flotation size bubbles', *J. Colloid Interface Sci.*, Vol. 109, pp.493–498.

Evans, L.F. (1954) 'Bubble-mineral attachment in flotation', *Industr. Eng. Chem.*, Vol. 46, No. 13, pp.2420–2424.

Gaudin, A.M. (1939) *Principles of Mineral Processing*, McGraw-Hill, New York.

Heide, B. (1963) 'Grundlagen der Zyklon Flotation', *Bergb. Wiss.*, Vol. 10, pp.152–168.

Kabanov, B. and Frumkin, A.Z. (1933) 'Uber die Gross electrolytisch entwickelter Grasblassen', *Phys. Chem. (Leipz.) A*, Vol. 165, pp.433–435.

Kinneberg, D.J. (1991) *Froth Flotation in an Air-Sparged Hydrocyclone*, Dissertation, Dept. Metallurgical Engineering, University of Utah, Salt Lake City, Utah.

Koczo, K., Koczone, J.K. and Wasan, D.T. (1994) 'Mechanisms for antifoaming action in aquaeous systems by hydrophobic particles and insoluble liquids', *J. Colloid Interface Sci.*, Vol. 166, pp.225–238.

Koczo, K., Lloyd, L. and Wasan, D.T. (1992) 'Effect of oil on foam stability: aqueous foams stabilized by emulsions', *J. Colloid Interface Sci.*, Vol. 150, pp.492–506.

Levich, V.G. (1962) *Physicochemical Hydrodynamics*, Prentice-Hall, Englewood Cliffs, NJ.

Miller, J.D. (1981) 'The concept of an air-sparged hydrocyclone', Presented at the *110th AIME Annual Meeting*, Chicago, February, pp.1–10.

Nguyen, A.V. and Schulze, H.J. (2004) *Colloidal Science of Flotation*, Marcel Dekker, New York, Basel.

Nguyen, A.V., Schulze, H.J., Stechemesser, H. and Zobel, G. (1997) 'Contact time during impact of a spherical particle against a plane gas-liquid interface: theory', *Int. J. Miner. Process.*, Vol. 50, pp.97–111.

Peck, W.H. (1922) *Centrifugal Apparatus (and Mode of Operating it) for Ore Flotation*, US Patent 1420138 19220620.

Philippoff, W. (1952) 'Some dynamic phenomena in flotation', *Trans. Amer. Inst. in. Eng. Min Eng.*, Vol. 193, April, pp.386–390.

Ralston, J., Dukhin, S.S. and Mishchuk, N.A. (2002) 'Wetting film stability and flotation kinetics', *Adv. Colloid Interface Sci.*, Vol. 95, pp.145–236.

Scheludko, A., Toshev, B.V. and Bojadjiev, D.T. (1976) 'Attachment of particles to a liquid surface (capillary theory of flotation)', *J. Chem. Soc., Faraday Trans.*, Vol. 72, pp.2815–2828.

Schulze, H.J. (1977a) 'New theoretical and experimental investigations on stability of bubble/particle aggregates in flotation: a theory on the upper particle size of floatability', *Int. J. Min. Processing*, Vol. 4, pp.241–259.

Schulze, H.J. (1977b) 'Dimentionless number and approximate calculation of the upper particle size of floatability in flotation machines', *Int. J. Min. Processing*, Vol. 9, No. 4, pp.321–328.

Schulze, H.J. (1983) *Physico-Chemical Elementary Process in Flotation*, Elsevier, Amsterdam, p.320.

Schulze, H.J. (1989) 'Hydrodynamics of bubble-mineral particle collisions', *Miner. Process. Extract., Met. Rev.*, Vol. 5, pp.43–76.

Schulze, H.J., Radoev, B., Geidel, T., Stechemesser, H. and Töpfer, E. (1989) 'Investigations of the collision process between particles and gas bubbles in flotation – a theoretical analysis', *Int. J. Miner. Process.*, Vol. 27, pp.263–278.

Sutherland, K. (1948) 'Physical chemistry of flotation. XI. Kinetics of the flotation process', *J. Phys. Chem.*, Vol. 52, pp.394–425.

Wark, I.W. (1933) 'The physical chemistry of flotation', *Int. J. Phys. Chem.*, Vol. 37, pp.623–644.

Ye, Y. and Miller, J.D. (1988) 'Bubble/particle contact time in the analysis of coal flotation', *Coal Prep.*, Gordon & Breach, Vol. 5, pp.147–166.

Ye, Y., Khandrika, S.M. and Miller, J.D. (1989) 'Induction-time measurements at a particle bed', *Int. J. Miner. Process.*, Vol. 25, pp.221–240.

Yoon, R.H. and Luttrell, G.H. (1989) 'The effect of bubble size on fine particle flotation', *Miner. Proc. Extract. Met. Rev.*, Vol. 5, pp.101–122.

Symbols

A	Dimensionless parameter
Ar	Archimedes number
B	Dimensionless parameter
C,C_1	Dimensionless numbers
E_c	Overall efficiency of encounter
E_i	Efficiency of encounter by interception
E_{in}	Efficiency of encounter by inertial impaction
E_{tur}	Efficiency of encounter by turbulent motions
F_b	Buoyancy force
F_{kT}	Entropy force
$f(R)$	Function dependent on surface mobility of air bubbles
g	Gravitational acceleration
k	Boltzman constant
L	Capillary length
M	Model parameter dependant on Reynolds number
N	Model parameter dependant on Reynolds number
O	Order of magnitude function
R_b	Bubble radius
$R_{b/o}$	Bubble or oil droplet radius

R_{oil}	Oil droplet radius
R_p	Particle radius
Re	Reynolds number
St	Stokes number
T	Absolute temperature
t_c	Collision contact time
t_{sl}	Sliding contact time
U	Bubble slip velocity
U_r	Bubble rise velocity
V	Relative velocity
V_S	Oil droplet settling velocity
We	Modified Weber number
X	Model parameter dependant on Reynolds number
Y	Model parameter dependant on Reynolds number
γ_{wg}	Surface tension of water or aqueous solution
δ	Flotation liquid density
ε	Volume fraction of the gas phase at low volume fraction of the oil phase
λ_k	Kolmogorov turbulent scale
μ	Liquid viscosity
ρ	Particle density
$\rho_{g/o}$	Density of air or oil
ρ_{oil}	Oil density
ρ_w	Water density
ϕ	Factor depending on the particle size
φ_0	Angle of the beginning of oil droplet sliding contact
φ_m	Angle of the end of oil droplet sliding contact